Limited Influence of P-Glycoprotein on Small-intestinal Absorption of Cilostazol, a High Absorptive Permeability Drug

HIDEKAZU TOYOBUKU,[1] IKUMI TAMAI,[1,2] KAZUYUKI UENO,[3] AKIRA TSUJI[1]

[1]Faculty of Pharmaceutical Sciences, Department of Pharmaceutical Biology, Kanazawa University, 13-1 Takara-machi, Kanazawa 920-0934, Japan

[2]Faculty of Pharmaceutical Sciences, Tokyo University of Science, Noda 278-8510, Japan

[3]National Cardiovascular Center, Osaka 565-8565, Japan

Received 26 February 2003; revised 13 May 2003; accepted 22 May 2003

ABSTRACT: Intestinal transport of the type III phosphodiesterase inhibitor cilostazol was characterized to evaluate the influence of secretory transporter. Intestinal absorption of cilostazol measured by the *in situ* closed loop method, showed regional differences, with high permeability in the upper part of the small intestine. Intestinal secretory transport of cilostazol at the ileum was tended to be decreased by the increase of tested concentration of cilostazol from 10 to 20 μM when evaluated by means of a Ussing-type chamber method with mounted rat intestinal tissues. Transcellular transport of cilostazol in the basolateral-to-apical direction in LLC-GA5-COL150 cells, which overexpress P-glycoprotein, was higher than that in parental LLC-PK1 cells. In addition, cilostazol reduced the basolateral-to-apical transport and increased the accumulation of [^{3}H]daunomycin in LLC-GA5-COL150 cells. Accordingly, cilostazol was demonstrated to be transported by P-glycoprotein, while cilostazol is not likely to cause induction of the expression level of P-glycoprotein by the same manner with rifampin. Apical-to-basolateral transport of cilostazol in Caco-2 cells was increased in a low concentration range, followed by a decrease with further increase of the concentration, while the permeability coefficient of cilostazol was above 1×10^{-6} cm/s at any concentration. Initial uptake of [^{14}C]cilostazol by Caco-2 cells was temperature dependent and was reduced in the presence of unlabeled cilostazol, suggesting that apical uptake is also mediated by a transporter(s). In conclusion, intestinal absorption of cilostazol, which has a high absorptive permeability, may not be significantly hampered by efflux transporters, such as P-glycoprotein. © 2003 Wiley-Liss, Inc. and the American Pharmacists Association J Pharm Sci 92:2249–2259, 2003

Keywords: P-glycoprotein; cilostazol; Caco-2 cells; secretion; transporter; influx; intestinal absorption

INTRODUCTION

Oral drug administration is generally preferred to treat chronic diseases. However, many drug candidates fail to fulfill their therapeutic potential owing to poor bioavailability as a result of low solubility, low permeability, and/or high metabolism. Among numerous factors that affect bioavailability, it is now generally recognized that active efflux of drugs by transporters and intestinal metabolism by enzymes should be considered to optimize oral bioavailability and to decrease variability at the absorption site.[1]

P-Glycoprotein (P-gp), which is a product of the mdr1 gene, was first characterized as the

Correspondence to: Akira Tsuji (Telephone: 81 76 2344478; Fax: 81 76 2344477; E-mail: tsuji@kenroku.kanazawa-u.ac.jp)

Journal of Pharmaceutical Sciences, Vol. 92, 2249–2259 (2003)

ATP-dependent transporter responsible for efflux of anticancer drugs from multidrug-resistant cancer cells.[2,3] P-gp is expressed not only on tumor cells, but also in a variety of normal tissues such as the kidney, liver, intestine, and endothelial cells of the blood–brain barrier.[4] P-gp is also known to govern the pharmacokinetics and tissue distribution of various drugs. In the intestine, P-gp is expressed on the apical membrane and acts as secretory pump to limit the absorption of various drugs.[5,6] Recently, it was demonstrated that a single nucleotide polymorphism in the MDR1 gene results in a significantly increased bioavailability of orally administered digoxin as a result of the decreased expression level of P-gp.[7] Therefore, efflux transporters such as P-gp could potentially be a determinant of bioavailability of many substrates.

Cilostazol is used to increase the intracellular level of cyclic AMP by blocking its hydrolysis by type III phosphodiesterase.[8] The Food and Drug Administration has approved cilostazol for treatment of intermittent claudication.[9] The principal mechanism of action is inhibition of platelet aggregation, thrombosis, and vasorelaxation by mediation of an increased cyclic AMP level.[10] Unlike other platelet aggregation inhibitors such as aspirin, cilostazol inhibits not only secondary platelet aggregation, but also ADP- and collagen-induced primary aggregation. Cilostazol also have the potential to reduce restenosis compared with optimal balloon angioplasty with aspirin or conventional coronary artery stenting with ticlopidine plus aspirin.[11] However, it was reported that intersubject variability in bioavailability of cilostazol following oral administration was relatively large, with a CV value of about 40 to 60% for most of the pharmacokinetic parameters.[12,13] Because cilostazol is a poorly soluble drug and the solubility may be one of causes for the large variability in bioavailability, the reasons for the variability are not clearly understood. It is important to understand the factors that affect the intestinal absorption of cilostazol, because such information will be helpful both in clinical use and for the optimization of drug design to reduce large intersubject variability in absorption after oral administration.

In the present study, we evaluated *in situ* absorption and *in vitro* intestinal tissue permeability of cilostazol in rats to investigate whether absorptive and/or secretory transporters are involved in cilostazol absorption from the gastrointestinal tract. In addition, we examined the transport mechanism of cilostazol by cultured monolayers of human MDR1 cDNA-transfected LLC-PK1 cells and Caco-2 cells, which express human MDR1 protein and other intestinal transporters.

MATERIALS AND METHODS

Materials

Unlabeled cilostazol and [^{14}C]cilostazol (29.3 mCi/mmol) were generously supplied by Otsuka Pharmaceutical Co. Ltd. (Tokushima, Japan). Unlabeled cilostazol was dissolved in ethanol as a 0.27-mM stock solution. [^{3}H]Daunomycin (18.5 Ci/mmol) was purchased from Perkin-Elmer Life Sciences, Inc. (Boston, MA). The protein assay kit was purchased from Bio-Rad (Melville, NY). Fetal calf serum (FCS) was obtained from Gibco-BRL (Grand Island, NY). LLC-PK1 or LLC-GA5-COL150 cells[14,15] were obtained from Riken Cell Bank (Tsukuba, Japan). Caco-2 and LS180 cells were obtained from American Type Culture Collection (Manassas, VA). All other chemicals were commercial products of reagent grade.

Animals

Male Sprague-Dawley rats weighing 220 to 250 g (Nihon-Clea, Tokyo, Japan) used in this study had free access to food and water. All the animal experiments were performed according to the Guidelines for the Care and Use of Laboratory Animals in Takara-machi Campus of Kanazawa University.

In Situ Closed Loop Method

Male Sprague-Dawley rats weighing 220 to 250 g (Nihon-Clea, Tokyo, Japan) were anesthetized with intramuscular administration of urethane (1.5 g/kg of body weight). An abdominal incision was carefully made to expose the intestinal tissue, which was divided into three segments—duodenum, jejunum, and ileum—each of 14-cm length. The intestinal contents were expelled from the respective segments and the segments were flushed with prewarmed (37°C) isotonic phosphate-buffered saline. Following this procedure, 0.7 mL of cilostazol (50 μM) in 2-(*N*-morpholino)ethanesulfonic acid (MES) buffer (5 mM KCl, 100 mM NaCl, 10 mM MES, 85 mM mannitol, polyethylene glycol 0.01%; pH 6.0; osmolarity, 290 mOs/kg) containing 1% bovine serum albumin (BSA) was introduced into a divided segments and both ends of the segment were ligated. The intestinal

segment was kept in the body for 20 min during the absorption experiments with a heating lamp to maintain the temperature of the preparation at 37°C. After 20 min, the luminal solution in the loop was collected and the loop was rinsed with isotonic MES buffer (5 mM KCl, 100 mM NaCl, 10 mM MES, 85 mM mannitol, polyethylene glycol 0.01%; pH 6.0; osmolarity, 290 mOs/kg) to give a total solution volume of 25 mL. The remaining amount of cilostazol in the intestinal lumen was determined by high-performance liquid chromatography (HPLC) to estimate the amount of unabsorbed cilostazol. The absorption of cilostazol was evaluated by the percentage of dose absorbed, by subtracting the remaining amount from the administered amount.

Ussing-Type Chamber Method

Rat ileal tissue sheets were prepared as described in our previous article.[16] The tissue preparation, consisting of the mucosa and most of the muscularis mucosa, was made by removing the submucosa and tunica muscularis with fine forceps. The tissue sheets were mounted vertically in a Ussing-type chamber that provided an exposed area of 0.5 cm^2. The volume of bathing solution on each side was 5 mL, and the solution temperature was maintained at 37°C in the water-jacket reservoir. Test solution (5 mL), with or without cilostazol (10 or 20 μM), was added to the donor or acceptor compartment, respectively. The duration of the transport experiment was 120 min. Samples (0.4 mL) were taken from the acceptor chamber at designated times and replaced with the same volume of drug-free test solution. The test solution was composed of 128 mM NaCl, 5.1 mM KCl, 1.4 mM $CaCl_2$, 1.3 mM $MgSO_4$, 21 mM $NaHCO_3$, 1.3 mM KH_2PO_4, and 10 mM NaH_2PO_4 at pH 7.4, and the solution was gassed with 95% O_2/5% CO_2 before and during the transport experiment.

Cultivation of LLC-PK1, LLC-GA5-COL-150, Caco-2, and LS180 Cells

LLC-PK1 and LLC-GA5-COL150 cells[14,15] were grown in M199 medium (Sigma, St. Louis, MO) supplemented with 10% FCS, 14.3 mM $NaHCO_3$, and 3% L-glutamine, without or with 150 ng/mL colchicine under 5% CO_2/humidified air at 37°C, as described previously.[17] For the transport experiments, LLC-PK1 and LLC-GA5-COL150 cells were seeded on Transwell microporous polycarbonate membrane (Costar, Cambridge, MA) at cell densities of 4×10^5 and 5×10^5 cells/cm^2, respectively, and cultured for 3 or 4 days before use.

Caco-2 cells were grown routinely in Dulbecco's modified Eagle's medium (GIBCO, Grand Island, NY) containing 10% FCS and 1% non-essential amino acids, 2 mM L-glutamine, 100 units/mL penicillin G and 100 μg/mL streptomycin under 5% CO_2/humidified air at 37°C, as described previously.[18] For the transport experiments, Caco-2 cells were grown on Transwell microporous polycarbonate membrane (Costar, Bedford, MA) and cultured for about 3 weeks prior to the transport experiments. For the uptake experiments, Caco-2 cells were seeded on culture dishes coated with rat tail collagen (Collaborative Research Inc., Grand Island, NY, USA) and grown for about 2 weeks.

LS180 cells were grown in MEM medium (Dainippon Pharmaceutical, Co., Ltd., Osaka, Japan) containing 10% FCS under 5% CO_2/humidified air at 37°C. For the experiment on induction of MDR1 mRNA with test compounds, LS180 cells were seeded on six-well culture dishes at a cell density of 2.6×10^6 cells/mL. When the cells reached 80% confluence, the medium was replaced with medium containing a test compound and the cells were grown for 24 h.

Uptake and Transport Experiments with Cultured Cells

The transport study was performed with LLC-PK1, LLC-GA5-COL150, and Caco-2 cells grown on Transwells (surface area; 1 cm^2) as described previously.[18] The confluent cells were washed with Hanks' balanced salt solution (HBSS, 0.952 mM $CaCl_2$, 5.36 mM KCl, 0.441 mM KH_2PO_4, 0.812 mM $MgSO_4$, 136.7 mM NaCl, 0.385 mM Na_2HPO_4, 25 mM D-glucose, and 10 mM *N*-2-hydroxyethylpiperazine-*N*′-2-ethanesulfonic acid (HEPES), pH 7.4; 315 mOs/kg), and 0.5 mL and 1.5 mL aliquots were added on the apical and basolateral sides, respectively, of a cell insert. To measure apical-to-basolateral or basolateral-to-apical flux, a test compound was included on the apical or basolateral side, respectively. At the designated time, 0.5 mL of basolateral or 0.2 mL of apical side solution was withdrawn and replaced with an equal volume of HBSS.

For accumulation studies with LLC-PK1 and LLC-GA5-COL150 cells, the medium was removed by aspiration at the end of the incubation period, and the monolayers were rapidly washed

twice with 2 mL of ice-cold incubation medium on each side. The filters with monolayers were detached from chambers, the cells on the filter were solubilized with 0.5 mL of 5 N NaOH, and the radioactivity in aliquots of 50 μL were counted. The radioactivity of the collected medium and the solubilized cell monolayers was determined in 4 mL of liquid scintillation cocktail, Cleasol-I (Nakalai Tesque, Kyoto, Japan) by liquid scintillation counting.

For the uptake experiments with Caco-2 cells, cells were seeded on four-well collagen-coated culture dishes and grown for about 2 weeks. Uptake of cilostazol by cultured monolayers of Caco-2 cells was examined by use of the method reported previously.[18] Cultured cells were first washed three times with 1 mL of HBSS adjusted to pH 7.4 by HEPES (10 mM) at 37°C. Uptake was initiated by adding 250 μL of incubation solution containing a test compound to the cells (usually 0.34 μM). At designated times, the cells were washed three times with 1 mL of ice-cold HBSS to terminate the uptake. To solubilize cells, 250 μL of 5 N NaOH was added and the mixture was left at room temperature for 2 h. After neutralization with 250 μL of 5 N HCl, the content of test compounds in the cell precipitate was measured with a liquid scintillation counter. Cellular protein content was measured by the method of Bradford using Bio-Rad protein assay kit with BSA as a standard.[19]

Real-Time Polymerase Chain Reaction

Total RNA was extracted from LS180 cells cultured for 4 days after having been washed with phosphate-buffered saline (PBS) using an RNeasy mini kit (QIAGEN Inc., Valencia, CA) according to the instructions provided by the manufactures. Single-stranded cDNA was made from 2.5 μg of total RNA by reverse transcription (RT) using an oligo dT primer. The sequences of the specific primers for target genes were as follows: the sense sequence was 5′-GCTCCTGACTATGCCAAAGC-3′ and the antisense sequence was 5′-ATTAG-GCCTTCCGTGCTGTA-3′ for MDR1: the sense sequence was 5′-AAGAGATGGCCACGGCTGCT-3′ and the antisense sequence was 5′-TCCTTC-TGCATCCTGTCGGC-3′ for β-actin. Quantitative real-time polymerase chain reaction (PCR) was performed using LightCycler® (Roche Diagnostics, Basel, Switzerland). PCR amplification was performed in a total volume of 10 μL containing 1 μL of cDNA sample, 0.5 μM forward and reverse primers and 1 μL LightCycler-DNA Master SYBR Green I (Roche Diagnostics, Basel, Switzerland). The initial amount of target mRNA in each sample was estimated from the experimental PCR threshold cycle (Ct) value with a standard curve generated using known amounts of plasmid DNA. β-Actin mRNA was also measured as an internal control. The PCR was performed as follows. MDR1: 45 cycles of 95°C for 0 s and combined annealing-extension at 56°C for 0 s and 72°C for 5 s after preincubation at 95°C for 10 min. β-Actin: 45 cycles of 95°C for 0 s and combined annealing-extension at 60°C for 0 s and 72°C for 12 s after preincubation at 95°C for 10 min.

Assay Procedures

For radioactive compounds, all samples were mixed with 4 mL of liquid scintillation cocktail, Cleasol-I. Radioactivity was determined using a liquid scintillation counter (LSC-1000, Aloka Co. Ltd., Tokyo, Japan). Nonradioactive cilostazol was measured by HPLC. The HPLC system was equipped with a constant flow pump (FP-2080 Plus; Japan Spectroscopic Co., Kyoto, Japan), a UV detector (UV-2075; Japan Spectroscopic Co., Kyoto, Japan), an integrator (Chromatopac CR3A; Shimadzu Co., Kyoto, Japan), and an automatic sample injector (AS-1555-10; Japan Spectroscopic Co., Kyoto, Japan). The analytical conditions used were as follows: the analytical column was STR-ODSII (4.6 mm × 25 cm, Shimadzu Co., Kyoto, Japan). The mobile phase was water–acetonitrile (60:40), at a flow rate of 1.5 mL/min. The detection wavelength for cilostazol was 254 nm.

Uptake (μL/mg protein) was evaluated by dividing the amount transported (dpm/mg protein) by the initial concentration of test compound on the donor side (dpm/μL). The permeability coefficient (μL/cm^2/min or cm/s) was obtained from the slope of the initial linear portion of the plots of permeation against time. All data are expressed as means ± SEM, and statistical analysis was performed by use of Student's *t*-test or Dunnett's test when multiple comparisons were needed. The criterion of significance was taken to be $p < 0.05$.

RESULTS

Regional Differences of Cilostazol Absorption and Transport in Rat Intestinal Tissue

The absorption of cilostazol was estimated in terms of disappearance from the rat intestinal

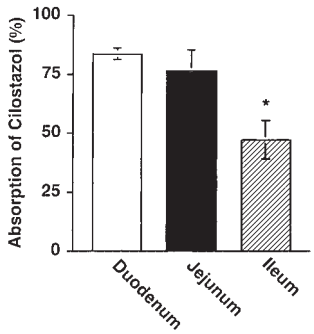

Figure 1. Cilostazol absorption from various regions of rat small intestine evaluated by the closed loop method. In the closed loop method, 0.7 mL of isotonic MES buffer containing 50 μM cilostazol (pH 6.0) was injected into a 14-cm long duodenum, jejunum, or ileum loop. Luminal fluid in each loop was collected 20 min after administration. Each value represents the mean ± SEM of four or five experiments. *Significantly different from the duodenum value by Student's *t*-test ($p < 0.05$).

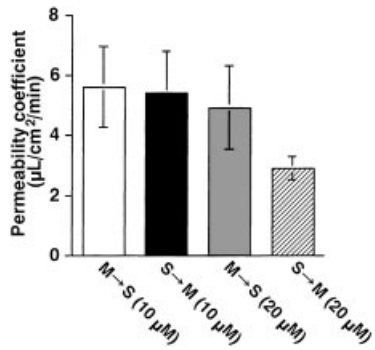

Figure 2. Permeation of cilostazol across isolated rat ileal tissue. Permeation of cilostazol was evaluated by use of a Ussing-type chamber method. The experimental solution was adjusted to pH 7.4 and the temperature was maintained at 37°C. Open and closed columns represent the permeation coefficient of 10 μM cilostazol in the mucosal-to-serosal and serosal-to-mucosal directions, respectively. Gray and hatched columns represent the permeation coefficient of 20 μM cilostazol in the mucosal-to-serosal and serosal-to-mucosal directions, respectively. Each value represents the mean ± SEM of three or five experiments. Key: (M-S): mucosal-to-serosal; (S-M): serosal-to-mucosal.

closed loop in 20 min. The fraction lost in 20 min ranged from 47.2% to 83.4% (Figure 1), decreasing in the order of duodenum ≅ jejunum > ileum. Thus, absorption from the upper segment of the small intestine was greater.

We next examined whether efflux transport of cilostazol occurs in rat ileal tissue by using the Ussing-type chamber method. Transport of cilostazol across a rat ileal sheet mounted on the chamber was measured in the mucosal-to-serosal and serosal-to-mucosal directions, and the permeability coefficient was obtained as the slope of the time course of appearance of intact cilostazol in the serosal or mucosal bathing solution, respectively. As shown in Figure 2, there was essentially no difference between the values of mucosal-to-serosal and serosal-to-mucosal permeations at 10 μM cilostazol. In contrast, the serosal-to-mucosal transport at 20 μM was tended to be lower than that at 10 μM, although the difference was not statistically significant.

Inhibitory Effect of Cilostazol on Daunomycin Transport and Accumulation

To investigate the interaction of cilostazol with P-glycoprotein, the inhibitory effect of cilostazol on the transport and accumulation of [^{3}H]daunomycin, a substrate of P-gp,[20] was examined in LLC-PK1 cells and LLC-GA5-COL150 cells, which overexpress P-glycoprotein on the apical membrane. As shown in Table 1, the trasncellular transport of daunomycin from the basolateral to apical side was significantly inhibited by cilostazol at 10 μM. On the other hand, the transport of [^{3}H]daunomycin from the apical to basolateral side was tended to be increased in the presence of 0.1 to 10 μM cilostazol. These changes in [^{3}H]daunomycin transport were not observed in LLC-PK1 cells. The cellular accumulation of [^{3}H]daunomycin from both the apical and basolateral sides was increased in LLC-GA5-COL150 cells in the presence of cilostazol (Figure 3). When uptake of [^{3}H]daunomycin by the LLC-GA5-COL150 cells was examined using cyclosporin A as the P-glycoprotein inhibitor, the similar increase was observed (data not shown). Accordingly, the effect of cilostazol on [^{3}H]daunomycin transport strongly suggested that cilostazol interacts with P-gp.

Transcellular Transport of Cilostazol across LLC-PK1/LLC-GA5-COL150 Cells

To examine directly whether cilostazol is a substrate for P-glycoprotein, we measured the transcellular transport of cilostazol by LLC-GA5-COL150 cells and parental LLC-PK1 cells. The basolateral-to-apical transport of cilostazol in LLC-PK1 monolayers was larger than that in the opposite direction (Figure 4). However, in LLC-GA5-COL150 cells, the basolateral-to-apical permeation of cilostazol was even greater than that

Table 1. Effect of Unlabeled Cilostazol on the Transcellular Transport of [^{3}H]Daunomycin by LLC-PK1 and LLC-GA5-COL150 Cells

	Permeability Coefficient (μL/cm^2/min)			
	LLC-PK1		LLC-GA5-COL150	
Cilostazol (μM)	A-to-B	B-to-A	A-to-B	B-to-A
Control	0.88 ± 0.10	1.23 ± 0.04	0.40 ± 0.03	2.10 ± 0.08
0.1	0.82 ± 0.06	1.23 ± 0.01	0.45 ± 0.02	2.02 ± 0.17
1.0	0.82 ± 0.08	0.91 ± 0.01[a]	0.45 ± 0.01	2.32 ± 0.17
10.0	0.79 ± 0.04	0.84 ± 0.05[a]	0.50 ± 0.03	1.42 ± 0.08[a]

Transport of [^{3}H]daunomycin (1 μM) across LLC-PK1 and LLC-GA5-COL150 monolayers was evaluated from the time course of amount transported to the receiver side in the apical-to-basolateral (A-to-B) and basolateral-to-apical (B-to-A) direction. Unlabeled cilostazol was added into the medium on both sides of the cell monolayers. Each datum represents the mean ± SEM of three experiments.

[a]Significantly different from the control value by Dunnett's test ($p < 0.05$).

in LLC-PK1. In contrast, apical-to-basolateral permeation in LLC-GA5-COL150 cells was smaller than that in LLC-PK1 cells. Thus, basolateral-to-apical-directed transport of cilostazol occurred in LLC-GA5-COL150 cells, demonstrating that cilostazol is a substrate of P-gp. In Figure 3, 10 μM cilostazol exhibited inhibitory effect on P-glycoprotein, resulting in an increased accumulation of [^{3}H]daunomycin. The observation of asymmetrical transport of cilostazol in LLC-GA5-COL150 cells, which is presumably mediated by P-glycoprotein, suggested that 10 μM of cilostazol was not enough to inhibit P-glycoprotein completely.

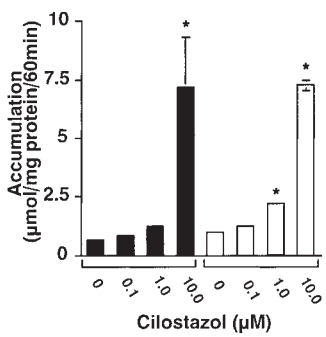

Figure 3. Effect of cilostazol on cellular accumulation of [^{3}H]daunomycin by LLC-GA5-COL150 monolayers. The cells were incubated for 60 min at 37°C in HBSS (pH 7.4) with 54 nM [^{3}H]daunomycin in the presence of increasing concentrations of cilostazol from 0.1 to 10 μM. Solid and open columns represent the accumulation from the apical and from the basolateral sides, respectively. Each value represents the mean ± SEM of three experiments. *Significantly different from the control value by Dunnett's multiple comparisons test ($p < 0.05$).

Effect of Cilostazol on Expression of MDR1 mRNA in LS180 Cells

To investigate whether cilostazol induces MDR1 mRNA, we determined the expression level of MDR1 mRNA in LS180 cells in the presence of cilostazol by a quantitative real-time PCR method. In accordance with previous results,[20] treatment of the LS180 cells with 10 μM rifampin caused an increase of MDR1-mRNA expression by threefold over untreated cells (Figure 5). In contrast, no difference in the level of MDR1-mRNA relative to the amount of β-actin mRNA was observed on treatment with cilostazol from 1.0 to 10 μM for 24 h in LS180 cells. Accordingly, cilostazol does not upregulate the expression of MDR1 gene in the same manner as rifampin.

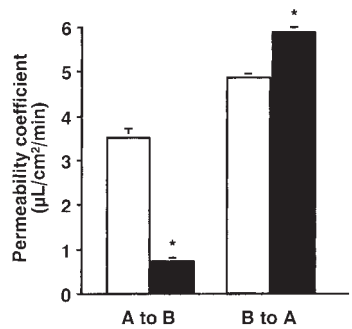

Figure 4. Transcellular transport of cilostazol by LLC-PK1 and LLC-GA5-COL150 monolayers. LLC-PK1 (open columns) and LLC-GA5-COL150 (solid columns) cells were incubated at 37°C with 10 μM cilostazol in HBSS buffer (pH 7.4). A to B and B to A represent apical-to-basolateral and basolateral-to-apical transport, respectively. Each point represents the mean ± SEM of three experiments.

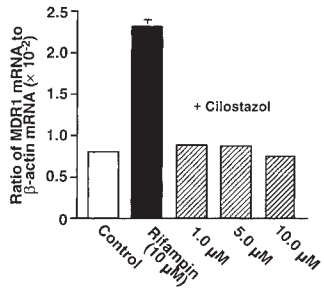

Figure 5. Expression level of MDR1 mRNA in LS180 cells after exposure to rifampin and cilostazol was assessed by real-time PCR analysis. Data represent expression level of MDR1 mRNA relative to the amount of β-actin mRNA. Open, solid, and hatched columns represent expression levels of MDR1 mRNA in non-treated, rifampin-treated, and cilostazol-treated LS180 cells. Each bar represents the mean ± SEM of three experiments.

Transcellular Transport of Cilostazol across Caco-2 Cells

To examine the transport mechanism of cilostazol across Caco-2 cells used as an intestinal model, transepithelial transport was measured at 10 μM cilostazol (Figure 6A). The transport of cilostazol was linear over 60 min. The basolateral-to-apical transport was about 1.5 times higher than the reverse one. The basolateral-to-apical efflux transport of cilostazol in Caco-2 cells was significantly inhibited by 10 μM cyclosporin A (a P-glycoprotein inhibitor), while the apical-to-basolateral transport of cilostazol was not affected.

The effect of increasing concentrations of cilostazol on the absorptive transport of cilostazol across a Caco-2 cells monolayer was studied. As shown in Figure 6B, apparent apical-to-basolateral transport of cilostazol increased as the cilostazol concentration was increased from 0.5 to 2 μM. At higher concentrations up to 10 μM, the apical-to-basolateral transport of cilostazol decreased. These results indicate the participation of a saturable influx transport process in Caco-2 cells.

Uptake of Cilostazol by Caco-2 Cells

To examine whether absorptive transporters participate in the transepithelial transport of cilostazol, apical uptake of [^{14}C]cilostazol by Caco-2 cells was examined by focusing on the temperature dependence and the inhibitory effect of several compounds. Figure 7A shows the time course of cilostazol uptake by Caco-2 cells at 37 or 4°C.

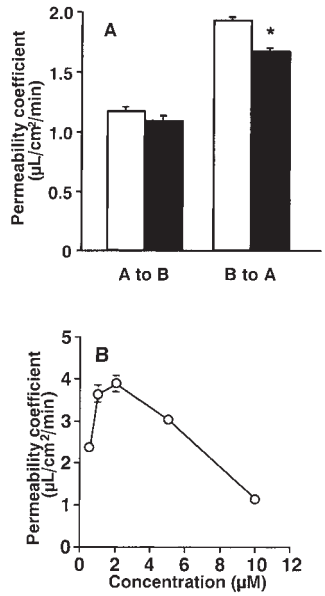

Figure 6. Transcellular transport of cilostazol by Caco-2 monolayers. (A) Permeability coefficient of 10 μM cilostazol was measured at 37°C in the absence (open columns) or presence (closed columns) of 10 μM cyclosporin A. A to B and B to A represent transport in the apical-to-basolateral and basolateral-to-apical directions, respectively. (B) Permeability coefficient of cilostazol at various concentrations in the apical-to-basolateral direction. Each point represents the mean ± SEM of three experiments.

Initial uptake of cilostazol up to 2 min was temperature dependent, with a significant change in uptake from 39.8 μL/mg protein/30 s to 2.8 μL/mg protein/30 s upon lowering the temperature from 37 to 4°C. To examine the possible involvement of influx transporter, inhibitory effects of several drugs on the initial uptake of [^{14}C]cilostazol (0.34 μM) were examined at 10 s, at which point uptake was linear and significantly temperature dependent. As shown in Figure 7B, significant reductions of the initial uptake of cilostazol by 1 mM cilostazol were observed, whereas other anionic compounds PAH probenecid and DIDS, cationic compounds N-methylnicotinamide (NMN), tetraethylammonium (TEA), verapamil, quinidine, and diphenhydramine, or a neutral compound, cyclosporin A were not inhibitory.

DISCUSSION

In the present study, we investigated whether absorptive and/or secretory transporters are involved in the intestinal transport of cilostazol

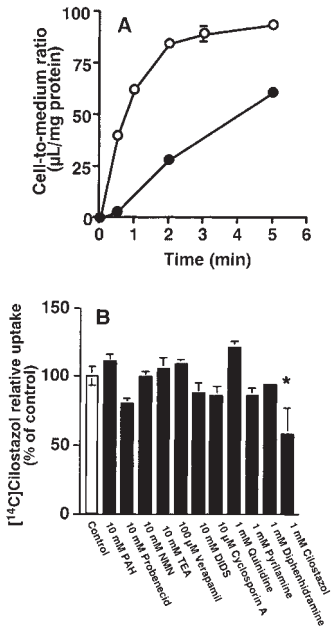

Figure 7. Effect of temperature and various drugs on the initial uptake of cilostazol by Caco-2 cells. (A) [^{14}C]Cilostazol (0.34 μM) uptake by Caco-2 cells was measured at pH 7.4 and 37°C (open circles) or 4°C (closed circles). (B) [^{14}C]Cilostazol (0.34 μM) uptake by Caco-2 cells was measured at pH 7.4 and 37°C for 10 s in the presence of several compounds. Each point represents the mean ± SEM of four experiments. *Significantly different from the control value by Dunnett's multiple comparisons test ($p < 0.05$).

to clarify the factors that affect its intestinal absorption.

Drug efflux mediated by transporters is reported to show regional differences, with an increase from the proximal to the distal intestine in animal models and humans.[22–25] Therefore, to investigate whether small intestinal regional difference exists in the absorption of cilostazol, we examined the absorption of cilostazol in rats by means of the intestinal-loop and the Ussing-chamber methods using ileal tissues (Figures 1 and 2). The absorption of cilostazol showed a clear regional difference, decreasing in the order of duodenum ≅ jejunum > ileum. The permeability in the serosal-to-mucosal direction in ileal tissue, measured by the Ussing-type chamber method, showed a tendency to be decreased with increase of cilostazol concentration. In our previous report, regional difference in the absorption of the quinolone antimicrobial grepafloxacin was also observed in the rat small intestine and was explained in terms of the involvement of multiple efflux transporters.[23,26] Therefore, these results suggest that region-dependent absorption/transport of cilostazol could be due to the participation of an efflux transporter(s).

Secretion of drugs mediated by P-glycoprotein is reported to increase from the proximal to the distal intestine in mice, rats, and humans.[22,27] Also, the level of MDR1-mRNA increases longitudinally along the intestine, with the lowest levels at the stomach and highest levels in the colon.[28] Therefore, to investigate the participation of P-glycoprotein in the secretory transport of cilostazol, we examined the inhibitory effect of cilostazol on the P-glycoprotein-mediated transport of daunomycin and the transport of cilostazol itself in the LLC-GA5-COL150 cell line, which overexpresses MDR1 (Figures 3 and 4). The basolateral-to-apical transport of daunomycin was inhibited by 10 μM cilostazol, accompanied with an increase in cellular accumulation of [^{3}H]daunomycin. Also, polarized transport of cilostazol was observed in LLC-GA5-COL150 cells. These findings directly demonstrated that the active efflux transporter P-glycoprotein is involved in the transport of cilostazol, and thus the region-dependent absorption of cilostazol mentioned above might be due to the participation of P-glycoprotein, at least in part.

MDR1 was recently shown to be transcriptionally regulated by pregnane X receptor (PXR).[29] It is possible that activation of MDR1 might alter the bioavailability of drug molecules. Greiner et al. reported that the plasma concentration of digoxin was reduced due to the induction of intestinal P-glycoprotein by coadministration of rifampin.[30] Therefore, we evaluated whether cilostazol induces the expression of MDR1 mRNA in LS180 cells, as a model of the induction of MDR1 gene via PXR. In the present study, rifampin induced the expression of MDR1-mRNA to a level about three times higher than the control in LS180 cells, which is consistent with previous reports.[21] In contrast, the expression level of MDR1 mRNA in LS180 cells treated with cilostazol up to 10 μM for 24 h was similar to that of the control (Figure 5). Therefore, it appears that cilostazol does not induce intestinal P-glycoprotein via PXR in LS180 cells, although the existence of other induction mechanisms that could not be observed in this cell line cannot be excluded.

We used Caco-2 monolayers to evaluate the transport mechanisms in intestinal epithelial cells. The vectorial transport of cilostazol across Caco-2 monolayers was observed at a concentration of 10 μM, with higher permeation in the basolateral-to-apical direction than in the reverse direction

(Figure 6A). The basolateral-to-apical transport of cilostazol was inhibited by 10 μM cyclosporin A, a P-glycoprotein inhibitor. Therefore, the region-dependent efflux observed in rat intestinal tissue may be explained by the participation of P-glycoprotein. Interestingly, concentration-dependent transport of cilostazol in the apical-to-basolateral direction was observed (Figure 6B). Apical-to-basolateral transport was increased from 0.5 to 2 μM, and at higher concentrations up to 10 μM its permeation was decreased to 50% of that at 0.5 μM. In our previous study, the 5-HT_3 receptor antagonist azasetron showed nonlinear intestinal absorption with an increase and a subsequent decrease in absorption as the concentration was increased.[31] The present results with Caco-2 cells are very similar to those previous observations. Therefore, cilostazol absorption may reflect the balance of absorptive and secretory processes, and P-glycoprotein may be one mediator of efflux transport.

To characterize the influx transporter, the initial uptake of [^{14}C]cilostazol into Caco-2 cells was studied. Initial uptake of cilostazol by Caco-2 cells was temperature-dependent (Figure 7A). The uptake of [^{14}C]cilostazol was reduced in the presence of 10 mM probenecid and 1 mM unlabeled cilostazol (Figure 7B). These results suggest that the absorption of cilostazol was carrier-mediated process, and further investigation will be needed to identify the putative absorptive transporter. Cilostazol may be metabolized in the process of absorption[32] and low solubility of cilostazol also affect the bioavailability. So, at present the factors that cause interindividual fluctuation in the bioavailability of cilostazol remain unclear. Influx and efflux transporters as well as metabolism and solubility could operate in concert to influence the bioavailability of cilostazol in a complex manner.

Many recent studies have indicated that secretory transporters such as P-glycoprotein can serve to limit the absorption of drugs across the intestinal epithelium. However, some compounds, such as azasetron, dexamethazone, digoxin, and grepafloxacin, exhibit bioavailabilities greater than 70%, despite the involvement of secretion by P-glycoprotein and/or MRP2.[31,33–36] In the case of cilostazol, the absorption is as high as 88.0% in rats despite the involvement of efflux transport by P-gp.[37] Artursson et al. reported that completely absorbed drugs have high permeability coefficients ($Papp > 1 \times 10^{-6}$ cm/s), while incompletely absorbed drugs have low permeability coefficients ($Papp < 1 \times 10^{-7}$ cm/s) in Caco-2 monolayers.[38] In the present study, the permeability coefficient of 10 μM cilostazol in the apical-to-basolateral direction was more than 1.92×10^{-5} cm/s. Theoretically, it was also shown that in the case of high permeability drugs, apparent permeability is hardly affected by P-gp.[39] Therefore, high absorption of drugs with high absorptive permeability can occur, even when the compounds are recognized by an efflux transporter in the small intestine. Care is necessary in the extrapolation of *in vitro* to predict *in vivo* absorption during drug discovery and development.

In conclusion, our findings demonstrate that cilostazol is transported by both secretory and absorptive transporters. P-Glycoprotein contributes in part to the intestinal secretion, while the absorptive mechanism has not been identified. Interaction of these mechanisms, and possibly also metabolism, could cause the large interindividual fluctuation in bioavailability of cilostazol. Our results suggest that the high absorption of cilostazol is due to its high absorptive permeability, and the participation of the efflux transporter P-glycoprotein does not retard the apparent intestinal absorption because of high absorptive membrane permeability by passive and/or carrier-mediated transport mechanisms.

REFERENCES

1. Wacher VJ, Silverman JA, Zhang Y, Benet LZ. 1998. Role of P-glycoprotein and cytochrome P450 3A in limiting oral absorption of peptides and peptidomimetics. J Pharm Sci 87:1322–1330.
2. Chen CJ, Chin JE, Ueda K, Clark DP, Pastan I, Gottesman MM, Roninson IB. 1986. Internal duplication and homology with bacterial transport proteins in the mdr1 (P-glycoprotein) gene from multidrug-resistant human cells. Cell 47:381–389.
3. Ueda K, Clark DP, Chen CJ, Roninson IB, Gottesman MM, Pastan I. 1987. The human multidrug resistance (mdr1) gene. cDNA cloning and transcription. J Biol Chem 262:505–508.
4. Tsuji A, Tamai I. 1997. Blood–brain barrier function of P-glycoprotein. Adv Drug Del Rev 25:287–298.
5. Schinkel AH, Wagenaar E, Van Deemter L, Mol CA, Borst P. 1995. Absence of the mdr1a P-glycoprotein in mice affects tissue distribution and pharmacokinetics of dexamethasone, digoxin, and cyclosporin A. J Clin Invest 96:1698–1705.
6. van Asperen J, Schinkel AH, Beijnen JH, Nooijen WJ, Borst P, van Tellingen O. 1996. Altered pharmacokinetics of vinblastine in mdr1a P-glycoprotein-deficient mice. J Natl Cancer Inst 88:994–999.

7. Hoffmeyer S, Burk O, von Richter O, Arnold HP, Brockmoller J, Johne A, Cascorbi I, Gerloff T, Roots I, Eichelbaum M, Brinkmann U. 2000. Functional polymorphisms of the human multidrug-resistance gene: Multiple sequence variations and correlation of one allele with P-glycoprotein expression and activity in vivo. Proc Natl Acad Sci USA 97:3473–3478.
8. Kimura Y, Tani T, Kanbe T, Watanabe K. 1985. Effect of cilostazol on platelet aggregation and experimental thrombosis. Arzneimittelforschung 35: 1144–1149.
9. Dawson DL, Cutler BS, Meissner MH, Strandness DE Jr. 1998. Cilostazol has beneficial effects in treatment of intermittent claudication: Results from a multicenter, randomized, prospective, double-blind trial. Circulation 98:678–686.
10. Tanaka K, Gotoh F, Fukuuchi Y, Amano T, Uematsu D, Kawamura J, Yamawaki T, Itoh N, Obara K, Muramatsu K. 1989. Effects of a selective inhibitor of cyclic AMP phosphodiesterase on the pial microcirculation in feline cerebral ischemia. Stroke 20:668–673.
11. Tanabe Y, Ito E, Nakagawa I, Suzuki K. 2001. Effect of cilostazol on restenosis after coronary angioplasty and stenting in comparison to conventional coronary artery stenting with ticlopidine. Int J Cardiol 78:285–291.
12. Ishida S, Morii M, Ueno K, Takada M, Sakata T, Okamoto A, Kobayashi J, Monta O, Koizumi N, Sasako Y, Shibakawa M. 2000. Studies on factor affecting pharmacokinetics of cilostazol and pharmacokinetics-pharmacodynamics analysis based platelet aggregation. Jpn J Hosp Pharm 26:264–272.
13. Bramer SL, Forbes WP, Mallikaarjun S. 1999. Cilostazol pharmacokinetics after single and multiple oral doses in healthy males and patients with intermittent claudication resulting from peripheral arterial disease. Clin Pharmacokinet 37:1–11.
14. Tanigawara Y, Okamura N, Hirai M, Yasuhara M, Ueda K, Kioka N, Komano T, Hori R. 1992. Transport of digoxin by human P-glycoprotein expressed in a porcine kidney epithelial cell line (LLC-PK1). J Pharmacol Exp Ther 263:840–845.
15. Ueda K, Okamura N, Hirai M, Tanigawara Y, Saeki T, Kioka N, Komano T, Hori R. 1992. Human P-glycoprotein transports cortisol, aldosterone, and dexamethasone, but not progesterone. J Biol Chem 267:24248–24252.
16. Tamai I, Takanaga H, Maeda H, Yabuuchi H, Sai Y, Suzuki Y, Tsuji A. 1997. Intestinal brush-border membrane transport of monocarboxylic acids mediated by proton-coupled transport and anion antiport mechanisms. J Pharm Pharmacol 49:108–112.
17. Kusunoki N, Takara K, Tanigawara Y, Yamauchi A, Ueda K, Komada F, Ku Y, Kuroda Y, Saitoh Y, Okumura K. 1998 . Inhibitory effects of a cyclosporin derivative, SDZ PSC 833, on transport of doxorubicin and vinblastine via human P-glycoprotein. Jpn J Cancer Res 89:1220–1228.
18. Tsuji A, Takanaga H, Tamai I, Terasaki T. 1994. Transcellular transport of benzoic acid across Caco-2 cells by a pH-dependent and carrier-mediated transport mechanism. Pharm Res 11:30–37.
19. Bradford MM. 1976. A rapid and sensitive method for the quantitation of microgram quantities of protein utilizing the principle of protein-dye binding. Anal Biochem 72:248–254.
20. Tanaka K, Hirai M, Tanigawara Y, Ueda K, Takano M, Hori R, Inui K. 1997. Relationship between expression level of P-glycoprotein and daunorubicin transport in LLC-PK1 cells transfected with human MDR1 gene. Biochem Pharmacol 53:741–746.
21. Schuetz EG, Beck WT, Schuetz JD. 1996. Modulators and substrates of P-glycoprotein and cytochrome P4503A coordinately up-regulate these proteins in human colon carcinoma cells. Mol Pharmacol 49:311–318.
22. Makhey VD, Guo A, Norris DA, Hu P, Yan J, Sinko PJ. 1998. Characterization of the regional intestinal kinetics of drug efflux in rat and human intestine and in Caco-2 cells. Pharm Res 15:1160–1167.
23. Naruhashi K, Tamai I, Inoue N, Muraoka H, Sai Y, Suzuki N, Tsuji A. 2001. Active intestinal secretion of new quinolone antimicrobials and the partial contribution of P-glycoprotein. J Pharm Pharmacol 53:699–709.
24. Tamura S, Ohike A, Ibuki R, Amidon GL, Yamashita S. 2002. Tacrolimus is a class II low-solubility high-permeability drug: The effect of P-glycoprotein efflux on regional permeability of tacrolimus in rats. J Pharm Sci 91:719–729.
25. Tian R, Koyabu N, Takanaga H, Matsuo H, Ohtani H, Sawada Y. 2002. Effects of grapefruit juice and orange juice on the intestinal efflux of P-glycoprotein substrates. Pharm Res 19:802–809.
26. Naruhashi K, Tamai I, Inoue N, Muraoka H, Sai Y, Suzuki N, Tsuji A. 2002. Involvement of multidrug resistance-associated protein 2 in intestinal secretion of grepafloxacin in rats. Antimicrob Agents Chemother 46:344–349.
27. Chianale J, Vollrath V, Wielandt AM, Miranda S, Gonzalez R, Fresno AM, Quintana C, Gonzalez S, Andrade L, Guzman S. 1995. Differences between nuclear run-off and mRNA levels for multidrug resistance gene expression in the cephalocaudal axis of the mouse intestine. Biochim Biophys Acta 1264:369–376.
28. Fojo AT, Ueda K, Slamon DJ, Poplack DG, Gottesman MM, Pastan I. 1987. Expression of a multidrug-resistance gene in human tumors and tissues. Proc Natl Acad Sci USA 84:265–269.

29. Geick A, Eichelbaum M, Burk O. 2001. Nuclear receptor response elements mediate induction of intestinal MDR1 by rifampin. J Biol Chem 276: 14581–14587.
30. Greiner B, Eichelbaum M, Fritz P, Kreichgauer HP, von Richter O, Zundler J, Kroemer HK. 1999. The role of intestinal P-glycoprotein in the interaction of digoxin and rifampin. J Clin Invest 104:147–153.
31. Tamai I, Saheki A, Saitoh R, Sai Y, Yamada I, Tsuji A. 1997. Nonlinear intestinal absorption of 5-hydroxytryptamine receptor antagonist caused by absorptive and secretory transporters. J Pharmacol Exp Ther 283:108–115.
32. Abbas R, Chow CP, Browder NJ, Thacker D, Bramer SL, Fu CJ, Forbes W, Odomi M, Flockhart DA. 2000. In vitro metabolism and interaction of cilostazol with human hepatic cytochrome P450 isoforms. Hum Exp Toxicol 19:178–184.
33. Toth GG, Kloosterman C, Uges DR, Jonkman MF. 1999. Pharmacokinetics of high-dose oral and intravenous dexamethasone. Ther Drug Monit 21: 532–535.
34. Iisalo E. 1977. Clinical pharmacokinetics of digoxin. Clin Pharmacokinet 2:1–16.
35. Efthymiopoulos C, Bramer SL, Maroli A. 1997. Pharmacokinetics of grepafloxacin after oral administration of single and repeat doses in healthy young males. Clin Pharmacokinet 33:1–8.
36. Yamaguchi H, Yano I, Saito H, Inui K. 2002. Pharmacokinetic role of P-glycoprotein in oral bioavailability and intestinal secretion of grepafloxacin in vivo. J Pharmacol Exp Ther 300:1063–1069.
37. Akiyama H, Kudo S, Shimizu T. 1985. The metabolism of a new antithrombotic and vasodilating agent, cilostazol, in rat, dog and man. Arzneimittelforschung 35:1133–1140.
38. Artursson P, Palm K, Luthman K. 2001. Caco-2 monolayers in experimental and theoretical predictions of drug transport. Adv Drug Del Rev 46:27–43.
39. Lentz KA, Polli JW, Wring SA, Humphreys JE, Polli JE. 2000. Influence of passive permeability on apparent P-glycoprotein kinetics. Pharm Res 17: 1456–1460.